

Axial anisotropic effects in hysteresis of $\pm J$ Ising lattices

M. C. Salas-Solis and F. Aguilera-Granja

Instituto de Física, Universidad Autónoma de San Luis Potosí, 78000 San Luis Potosí, S.L.P., Mexico

J. Cartes, S. Contreras, and E. E. Vogel

Departamento de Física, Universidad de La Frontera, Casilla 5 4-D, Temuco, Chile

(Received 18 November 2003; revised manuscript received 31 March 2004; published 5 August 2004)

Anisotropy is added to the Edwards-Anderson model in such a way that interactions along the x axis are stronger by a factor f with respect to other interactions. Hysteresis cycles for square and cubic $\pm J$ Ising spin glasses are obtained by Monte Carlo simulations. Concentration x of ferromagnetic interactions ($-J$), temperature T , and f are varied to study their effects on the characteristics of the hysteresis loops. Several behaviors are simulated and compared to experimental curves, finding similarities. Important aspects such as virgin curve, remnant magnetization, and coercive field are discussed in detail. It is found that anisotropy tends to stabilize spin-glass phases, leading to a larger remnant magnetization and larger coercive field.

DOI: 10.1103/PhysRevB.70.064404

PACS number(s): 75.30.Gw, 75.50.Lk, 75.60.Ej

I. INTRODUCTION

The Edwards-Anderson (EA) model¹ has been investigated for about three decades following several motivations. In these systems, ferromagnetic interactions ($-J$) in concentration x , and antiferromagnetic interactions ($+J$) in concentration $1-x$, are distributed at random in a lattice. Probably the main motivation has been the possible use of this model as a general guide towards most of the phenomena that characterize a spin glass.² Along this line of thought we present here the results on magnetic properties of $\pm J$ Ising square lattices (with some calculations for cubic lattices), where interactions (independent of the sign) are stronger along one direction with respect to the other(s) by a factor f .^{3,4} This establishes a geometrical anisotropy affecting the magnetic interactions and having a deep influence on the spin-glass properties of the EA model. Thus, for instance, it has been found^{3,5} that ground-state energy lowers, degeneracies decrease, and site-order parameters increase upon increasing f , thus making more stable a possible spin-glass phase.

Then, it is possible to think that a larger stability on the spin-glass behavior will also show in magnetic properties of the systems. In particular, magnetization in the presence of an external magnetic field, reflecting competition of several realizations of internal local fields with the externally applied magnetic field, would give rise to a rich phenomenology worth of studying. This is the main purpose of this paper.

Very little is known with respect to the anisotropy effects on the hysteresis loops of these systems. It is known that simulations of hysteresis curves^{6,7} of $\pm J$ Ising lattices produce sectors very similar to those found in some real systems.^{8,9} Preliminary results⁴ show that hysteresis curves of anisotropic $\pm J$ Ising lattices present wiggles, or small jumps, as it is found in some real systems where frustration occurs.¹⁰ The energy dissipated per cycle (area within the hysteresis loop) increases with the anisotropy factor, which is in good correspondence with the larger values for order parameters under the same conditions.

In the present paper we want to extend this study to answer the following questions related to isotropic and aniso-

tropic magnetic hysteresis simulations on the EA model: Is it possible to simulate the virgin curve outside the main loop as in many spin glasses?⁸ What are the main features of the low-temperature hysteresis curves as functions of f ? What is the behavior of the coercive field upon variation of both anisotropy factor f and temperature T ? What is the behavior of the remnant magnetization as functions of f and T ? What is the role of x , the concentration of ferromagnetic interactions? How do hysteresis curves change shape upon varying x in its range $[0,1]$? In answering these and other possible questions we will bear in mind the behavior of some real spin-glass systems.⁸⁻¹¹

The paper is organized as follows. In Sec. II we give a formal presentation of the model focusing on the anisotropy factor f . In Sec. III we present the main results and discuss some of their most important features. Finally, in Sec. IV we make a summary of the main conclusions.

II. THEORY AND DEFINITIONS

Let us consider a spin S_{ij} at site ij of a square lattice (SL) with coordination number $Z=4$ and a total of $L_x \times L_y = N$ sites, all occupied by Ising one-half spins. We assume periodic boundary conditions and a homogeneous magnetic field B applied to the lattice. Interactions among spins can be either ferromagnetic (F) in proportion x , or antiferromagnetic (AF) in proportion $1-x$. In the present paper we introduce an anisotropy to the local fields such that interactions along the direction x have the strength f_x , which is in general different from interaction along the direction y with the strength f_y .

Such a system is described by an Ising Hamiltonian,

$$H = H_x + H_y - B \sum_{j=1}^{L_y} \sum_{i=1}^{L_x} S_{ij}, \quad (1)$$

where the asymmetric components are written as

$$H_x = f_x \sum_{j=1}^{L_y} \sum_{i=1}^{L_x} J_{ijx} S_{ij} S_{i+1j}, \quad (2)$$

$$H_y = f_y \sum_{i=1}^{L_x} \sum_{j=1}^{L_y} J_{ijy} S_{ij} S_{ij+1}. \quad (3)$$

Exchange interactions J_{ijx} and J_{ijy} can take values either $=-J$ (F) or $+J$ (AF), with $J>0$. In these units B , temperature T , and total energy E are measured in units of J . It is convenient to define a relative anisotropy factor $f=f_x/f_y$, which we will use from here on. The extension to a simple cubic lattice (CL) with $Z=6$ is straightforward, with $f_z=f_y$.

For a given concentration x , different systems are possible, according to the distribution of bonds through the lattice. A sample is a random distribution of bonds that is kept frozen and stored. Then, for each such sample, different anisotropic realizations are achieved by simply varying f in the range from 1.0 to any high anisotropic value. In the present paper we scan up to $f=12$.

For a given sample, the magnetization per site is

$$m(B, dB/dB|, T, f) = \frac{1}{N} \sum_{i=1}^N S_i, \quad (4)$$

where $dB/dB|=-1$ ($+1$) for decreasing (increasing) B .

Hysteresis curves for isotropic lattices have been previously reported.^{6,7,12} We present here a systematic study based on hysteresis simulations for anisotropic SLs. Emphasis of the presentation will be on low-temperature (LT) hysteresis behavior of SLs upon variations of f and x . This treatment can be easily extended to CLs, which we do to study the behavior of the virgin curve (VC) in the original isotropic samples.

Simulations are done as follows: A system (SL or CL) and a size N are chosen. Five hundred random samples are then considered in sequential order. For each sample a new calculation is started for each f value. B is treated as an independent variable and will be varied in steps of dB equivalent to flipping one spin at a time. For each value of B the energy is thermalized by means of a Monte Carlo (MC) calculation with the Metropolis algorithm, over 10^4 MC steps.¹² Magnetization is evaluated and stored. Two different processes will be analyzed. For each sample, (1) several hysteresis cycles (including the virgin curve) are obtained, and (2) the first complete cycle is stored to perform statistics over 500 cycles, one for each sample.

It is well known that the MC method with the Metropolis algorithm faces difficulties for the particular case of $T=0.0$, $f=1.0$, and $x=0.5$. Special treatment has been developed to overcome this particular difficulty.^{13,14} However, most of our work is far from this particular point of the multidimensional parameter space to be considered below. It is worth noticing that upon the slightest anisotropy the accidental degeneracies are removed and a true ground-energy valley arises.^{3,5} Due to the previous argument we will stick to the MC method with the Metropolis algorithm through the entire parameter space.

The choice of MC steps was based on the reproducibility of the hysteresis loops. Since hysteresis measurements are essentially done upon varying magnetic field at a given temperature, it corresponds to an out-of-equilibrium experiment. Hence, results can vary depending on the speed at which magnetic field is changed. Eventually, if huge times are used

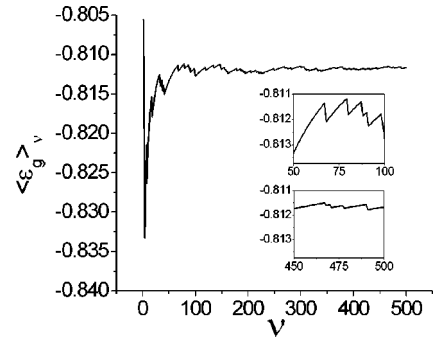


FIG. 1. Progressive average values for the ground-state energy per bond as a function of the number of samples used to obtain such averages. The upper inset shows the onset of stabilization for the range $50 < \nu < 100$; the lower inset shows a stabilized function for the range $450 < \nu < 500$.

between successive magnetic field variations, better equilibration can be achieved and the loop can tend to close. This, in fact, happens for the systems under study and eventually also for some real experiments for systems with strong competitions among interactions. On the other hand, if too short times are used, simulations depend on the seed of the MC process. We have made the decision of choosing an equilibration time that gives reproducible results independent of the initial seed and sequence of visited states. Such reproducible results could still be subject to small variations if longer times are used, however, this would affect all the results here in the same direction (tiny closing of the loops), which would still allow for the discussion of general tendencies on the other relaxation processes that produce larger effects (magnetic field and temperature variation). A set of 500 samples 12×12 , isotropic case, $T=0.1$, was studied systematically for the isotropic case (the less convenient case) increasing equilibration times between 100 MC steps through 100 000 MC steps. It is found that already at 1000 MC steps the loops are reproducible with negligible variations when they are run under different sequential conditions. Then, at 10 000 MC steps no variations on the shape of the loops are found within two significant digits of precision. Then we have used this equilibration time, 10^4 MC steps, through all simulations reported here.

The choice of the number of samples used to average over different disorder realizations was established after studying the stability of the results for several physical magnitudes that characterize these systems.^{15,16} In Fig. 1 we present progressive average values for the ground-state energy per bond $\langle \epsilon_g \rangle_\nu$, for ν samples with $\nu=1, 2, 3, \dots, 500$. We have used here the same 500 samples of size 12×12 with an anisotropy factor $f=3.0$. As it can be seen in the main body of Fig. 1 the average value of the energy oscillates strongly for a small number of samples ($\nu < 50$). Then, as the number of samples considered in the average increases the oscillations are dumped, showing the onset of convergence in the upper inset. Finally, for even larger values of ν the oscillations are strongly dumped to a desired degree of accuracy, as shown in the lower inset. We can conclude that convergence is fast and is even faster when f is increased. Convergence of other physical parameters was studied in a similar way for differ-

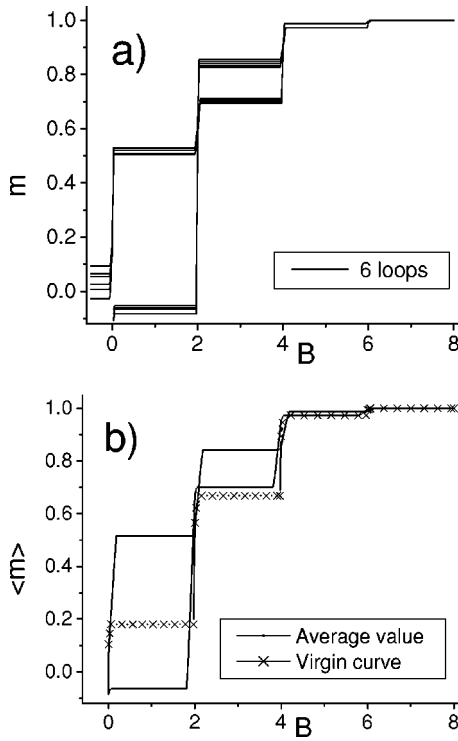


FIG. 2. Low-temperature virgin curve (VC) followed by six consecutive hysteresis loops for one isotropic $8 \times 8 \times 8$ sample. Notice that the VC lays outside of the loops, and that no return-point memory is observed. Both facts are actually observed for some real spin glasses.

ent temperatures.⁵ The worst convergence conditions are for the isotropic case and equal amounts of F and AF bonds, for which it was found that average values based on 300 samples are stable within two significant figures.^{15,16} Then, using 500 samples ensures reliable results throughout the entire parameter space.

Samples of different sizes were calculated. However, in the rest of the presentation we restrict ourselves to size $N = 12 \times 12$ due to highly demanding computer times and storage of data. No important size effects were observed for N larger than 8×8 , as will be shown below.

III. RESULTS AND DISCUSSION

Let us begin by considering a cubic lattice with $x=0.5$ (equal amounts of F and AF bonds) and $f=1.0$, namely, an isotropic case. As a first application we take $T=0.0001$ (considered true zero T as far as these simulations are concerned). The MC process begins at a random state (with magnetization close to zero) and no magnetic field. Then, B is slowly increased up to saturation, thus generating the so-called virgin curve (VC). Then B is slowly decreased up to saturation in the opposite sense, returning back to saturation for positive field closing a loop. This process is repeated as many times as needed. In Fig. 2 we present the VC and six consecutive hysteresis loops for one particular sample. In the upper part of Fig. 2(a) we present the six consecutive loops without the VC, emphasizing the first quadrant only ($B > 0$,

$m > 0$), with the aim of reaching a better resolution on the different loops. On the left-hand side of Fig. 2(a) a small portion with $B < 0$ can be seen, and we can clearly observe each one of the six paths corresponding to each one of the simulated loops. For the intervals $0 < B < 2$ and $2 < B < 4$ only five are observed. This number is reduced to one in the following step ($B > 4$). That is to say, for each field interval there are several possible magnetization values and some can be more frequently visited than others. A different way of phrasing the same phenomenon is by saying that no return-point memory (RPM) is observed. Such property is not guaranteed for systems with competing interactions, thus, in the case of random fields, in some cases RPM is obeyed¹⁷ and in other systems with competitive interactions, such property is absent.^{13,18}

In Fig. 2(b), we present the VC and the average hysteresis curve obtained from previous loops. As it can be noticed, the VC lays outside the main loop, which is particularly notorious for the interval $2 < B < 4$ in Fig. 2(b). This fact is actually observed for some real spin glasses.⁸ Such an interesting feature was reproduced by our simulations for most of our samples, both SLs and CLs.

From now on we report properties on SLs only, although similar behaviors are found also in CLs. Computer times needed for CLs are huge, compared to times needed in the case of SLs with a similar number of spins. Since all the phenomena are present in both lattices, focusing on the simple system (SL in this case) allows for an inclusion of more parameters which can be widely varied.

We now proceed to study variations of the LT hysteresis cycle for increasing values of f . The introduction of the anisotropy factor f , changes the energy scale, which affects the values of the magnetic field. In order to present hysteresis loops for different anisotropy factors within a common field framework, we introduce a convenient renormalization factor. Namely, the renormalized magnetic field B^* is defined as

$$B^*(f) = \frac{ZB}{2f + (Z-2)}. \quad (5)$$

In Fig. 3 we present hysteresis loops for different anisotropy factors as functions of the renormalized magnetic field B^* . Each curve is defined by average values over 500 samples of size 12×12 , at four different values of f ; namely, $f=1.0$ (isotropic), 1.5 (slightly anisotropic), 3.0 (anisotropic), and 6.0 (highly anisotropic). T is again 0.0001 and VCs are suppressed for clarity. Several comments are in order. First, simulations of LT hysteresis curves exhibit sectors within the loop (regulated by Z) as actually shown by some real spin-glass systems;^{8,9} In particular the closing of the loop at $B^* = 0.0$, due to cancellation of local fields, is also shown by simulations. Second, a small anisotropy ($f=1.5$) breaks loops and sectors into ladders of irregular step width and height; step width is governed by values of the external field coinciding with critical values of internal fields for which spin turnovers are possible, thus producing magnetization jumps. Such fields are $B^* = \pm 4.0, \pm(4f/f+1), \pm[4(f-1)/f+1], \pm 4/f+1$, and 0.0 (for $Z=4$). Third, simulations for SL lead to nine steps; however, in real systems irregularities in the lattice can

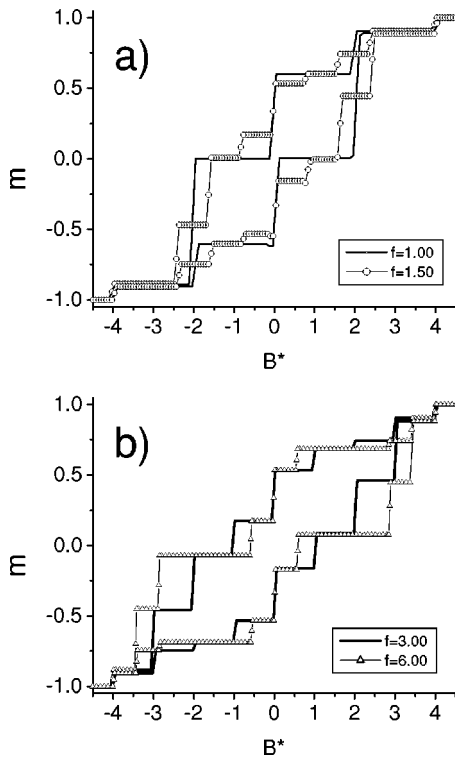


FIG. 3. Low-temperature average hysteresis curves over 500 samples 12×12 at four different anisotropy factors f and $x=0.5$, as functions of the renormalized field B^* . The different anisotropic factors correspond to the following cases: isotropic $f=1.0$, slightly anisotropic $f=1.5$, anisotropic $f=3.0$, and highly anisotropic $f=6.0$.

bring in more steps, or small wiggles, in the hysteresis loops.¹⁰ Fourth, the particular case of having all steps of the same width is obtained here for $f=3.0$. Fifth, for high anisotropy, the main effects are observed: (a) terraces of constant magnetization appear as shown in some real systems exhibiting mixed magnetism;¹⁹ (b) as f gets very large ($f=6.0$) two sectors tend to prevail, with the central point ($B \approx 0.0$) tending to close; and (c) for even higher values of f the closing effect continues, but there is always a remnant magnetization producing tiny steps in the central sector (this effect will be discussed in more detail in the next paragraph). Sixth, the magnitude of the renormalized coercive field increases for low f values, reaches a maximum, and then tends to diminish; such a strange behavior will be discussed below. Seventh, the area within the loop increases with f indicating that larger energy is required to overturn all spins, thus favoring a spin-glass phase.^{4,5} Eighth, as T first increases (not shown here) rounding effects appear on the steps of constant magnetization; for higher T steps slowly disappear leading to the usual inclined S -like shape hysteresis loops, which eventually closes for high enough T values.^{4,5}

Let us now discuss remnant magnetization $m(B=0)$ in a more detailed way using the notation introduced in Eq. (4). As B comes down from saturation, magnetization $m(B > 0, -1, T, f)$ decreases upon lowering B . Remnant magnetization is then defined as $m(0, -1, T, f)$. In Fig. 4 we present the remnant magnetization as a function of f , for several different values of T . Remnant magnetization decreases with T , as

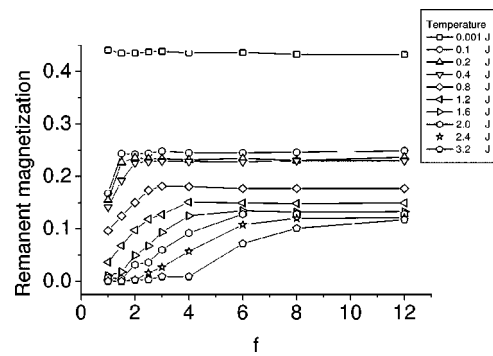


FIG. 4. Remnant magnetization as functions of anisotropy factor f and temperature T for $x=0.5$. The expected decrease of this magnitude with temperature tends to be somewhat compensated by large anisotropic factors.

can be expected. However, Fig. 4 also shows the stabilization role played by f , tending to reverse the effect of increasing T to some extent. This is due to the remanence of magnetization in the “horizontal” chains, as the frustration tends to accumulate on the weak “vertical” bonds.

Coercive field B_c is defined as the value of the field such that $m(B=-B_c, -1, T, f)=0$. In Fig. 5 we present the variation of the magnitude of the coercive field as function of T and f . In general terms B_c decreases with T , as can be anticipated. However, for low-anisotropy values ($f < 2$) an unexpected behavior is observed in the sense that as T increases from zero, B_c first increases before following the general trend of monotonous decrease for higher T values. The reason for this is that temperature induces the presence of a few random local weak fields, producing rounding effects in the hysteresis curves as T slightly increases. For higher values of T local fields are completely overcome, yielding basically free spins not leading to net magnetization. On the other hand, as f increases “horizontal” interactions become dominant, leading to rigid sectors of the lattice and making it harder for the external field to overturn solidary spins. This explains the increase of B_c as f increases.

To check the soundness of previous results based on the shape of the hysteresis curves corresponding to size 12

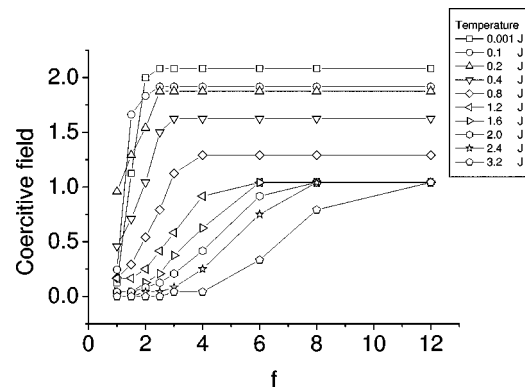


FIG. 5. Coercive field as a function of anisotropy f factor and temperature T for $x=0.5$. This characteristic parameter decreases with temperature in the long run, but it presents some fluctuations for small values of f .

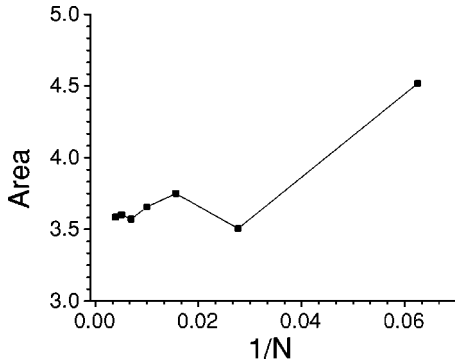


FIG. 6. Area under the hysteresis curves as a function of $1/N$ with $N=L \times L$ for different L values (4, 6, 8, 10, 12, 14, and 16) for $T=0.1$, $f=3.0$, and $x=0.5$.

$\times 12$, let us study the variation of the area under the hysteresis curves $\langle A(T, f) \rangle$ as a function of L , which defines the size of systems $L \times L$. Calculations are done at $T=0.1$ and for an anisotropic factor $f=3.0$. The area under the curve depends essentially on both remnant magnetization and coercive field, which is then an accurate measure for the characteristics of the hysteresis behavior. In Fig. 6 we plot $\langle A(0.1, 3.0) \rangle$ vs the reciprocal value of the system size ($1/N$) being $N=L \times L$ for 500 samples and $L=4, 6, 8, 10, 12, 14$, and 16. As it can be seen, size effects cease to be important for $1/N < 0.0156$ ($L > 8$), which justifies our choice of $N=12 \times 12$ in the present analysis. This is enough for the purpose of checking the stability of the results reported here, and we do not attempt a finite-size scaling analysis to extrapolate values towards the thermodynamic limit. On the other hand, using systems of sizes larger than 12×12 will need larger computer times without altering the main conclusions reached here.

Let us now turn our attention to the case of the variable x , which we present for the case of $f=3.0$ based on 500 samples 12×12 in Fig. 7. In the lower part of this figure we present results for the mostly AF samples, namely, $x=0.0, 0.2$, and 0.5 . In the upper part we report cases for the mostly F samples, namely, $x=0.5, 0.8$, and 1.0 (Case $x=0.5$, spin-glass like, is repeated for comparison purposes). T is always 0.0001 .

For $x=1.0$, a typical hysteresis loop for a ferromagnet is obtained, namely, one single loop with a rectangular shape. At $x=0.8$, some frustration is present in the system, so magnetization jumps occur at fixed values of B^* . At $x=0.5$, we recover the curve labeled $f=3.0$ in Fig. 3, which is included here to facilitate crossed analysis. At $x=0.2$, height of the steps decreases notoriously with a tendency of making the loop horizontal and closing it. At $x=0.0$, the loop is more horizontal and almost closed; however, it does not close at very low T due to the presence of different AF domains in the sample which are impossible to overturn at very low T .

It is very encouraging to compare curves for $0.70 < c < 0.95$ (only $x=0.8$ is shown in Fig. 7) to Fig. 1 of Ref. 19 and realize that there are some general similarities, such as vertical jumps and terraces. There are also some differences (such as increases of magnetization at fields different from those where magnetization decreases) that are not accounted for by our simple model.

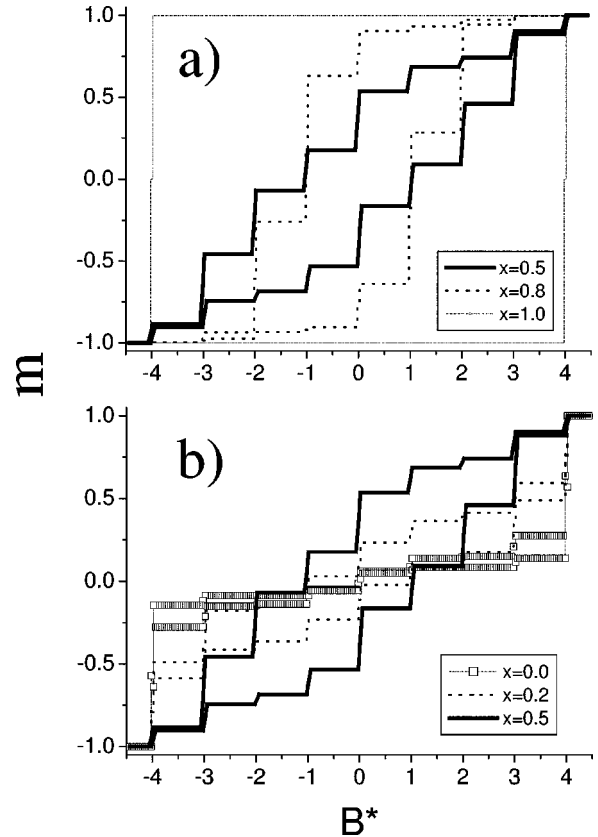


FIG. 7. Average hysteresis curves for 500 samples 12×12 at $f=3.0$ for different concentrations of ferromagnetic bonds x . In the lower part we include the mostly AF cases ($x \leq 0.5$), whereas in the upper part we present results for the mostly F cases ($x \geq 0.5$).

IV. CONCLUSIONS

The inclusion of anisotropy into the Edwards-Anderson model produces a large variety of hysteresis loops, which resemble several characteristics of measured hysteresis loops on different real systems.

Concluding remarks will be presented in an increasing order of the role of the anisotropy, beginning with the isotropic case. Thus for $f=1.0$, we can mention three main features. The VC can go outside the main loop as reported in frustrated systems.⁸ These systems present a complex configuration space, with many local energy minima leading to several possible paths for hysteresis loops. This is indeed found experimentally¹⁹ and it is also simulated by our MC calculations, as discussed in Fig. 2 above. Another characteristic of some frustrated systems is the presence of sectors in the hysteresis with the tendency of closing at the center ($B \approx 0$);^{8,9} this is a feature always reproduced by our simulations due to the discrete nature of the $\pm J$ Ising Hamiltonian of the Edwards-Anderson model.

The first consequence of introducing anisotropic interactions (as can be seen from Fig. 3 above) is the surge of several possible steps or terraces of constant magnetization at low T . This feature is also shown by several systems, in particular by alloys of $\text{Fe}_x\text{Mg}_{1-x}\text{Cl}_2$, where there are competing interactions of different strengths.¹⁹

Anisotropic interactions induce large remnant magnetization as well as large values for coercive field. This is due to the partial removal of the itinerant frustration that is present in the isotropic case. The overall consequence of this is a larger hysteresis loop for the anisotropic case, meaning a larger energy dissipated in the hysteresis cycle. Therefore, upon increasing f the spin-glass phase is favored.

When temperature is increased, simulations predict a quick decrease of both remnant magnetization and coercive field, as reported for some real systems with competing interactions, such as AuFe alloys.¹¹

A great variety of systems can be mimicked when the relative concentration between F and AF interactions is varied. This makes present treatment appropriate for gaining

some understanding in cases where several magnetic phases can coexist in the same material, as is the case of the doped perovskites for example.²⁰ However, modeling such complex real systems would require a more complete Hamiltonian than the one used in the present analysis.

ACKNOWLEDGMENTS

This work has been partially funded in Mexico by CONACyT proposal-2003, and PROMEC-CA230, and in Chile by FONDECYT under Contract Nos. 1020993, 1010511, and 7010511, and the Millennium Scientific Initiative under Contract No. P-02-054-F.

-
- ¹S. F. Edwards and P. W. Anderson, *J. Phys. F: Met. Phys.* **5**, 965 (1975).
- ²K. Binder and A. P. Young, *Rev. Mod. Phys.* **58**, 801 (1986).
- ³M. C. Salas-Solis, F. Aguilera-Granja, E. E. Vogel, and S. Contreras, *Physica A* **327**, 477 (2003).
- ⁴M.C. Salas-Solis, F. Aguilera-Granja, E. E. Vogel, and J. Cartes, *J. Alloys Compd.* **369**, 55 (2004).
- ⁵M. C. Salas-Sols, Ph.D. thesis, University Autónoma San Luis Potosí, Mexico, 2003.
- ⁶E. E. Vogel, J. Cartes, P. Vargas, D. Altbir, S. Kobe, T. Klotz, and M. Nogala, *Phys. Rev. B* **59**, 3325 (1999).
- ⁷E. E. Vogel, J. Cartes, P. Vargas, and D. Altbir, *Physica B* **284**, 1211 (2000).
- ⁸S. Senoussi, *J. Phys. (Paris)* **45**, 315 (1984).
- ⁹J. H. Zhang, F. Chen, J. Li, and C. J. O'Connor, *J. Appl. Phys.* **81**, 5283 (1997).
- ¹⁰A. Paduan-Filho, C. C. Becerra, V. B. Barbeta, Y. Shapira, J. Campo, and F. Palacio, *J. Magn. Magn. Mater.* **140**, 1925 (1995).
- ¹¹I. A. Campbell, S. Senoussi, F. Varret, J. Teillet, and A. Hamzić, *Phys. Rev. Lett.* **50**, 1615 (1983).
- ¹²E. E. Vogel, J. Cartes, D. Altbir, and P. Vargas, *J. Magn. Magn. Mater.* **226**, 1248 (2001).
- ¹³J. M. Deutsch and O. Narayan, cond-mat/0301083.
- ¹⁴E. E. Vogel, A. J. Ramirez-Pastor, and F. Nieto, *Physica A* **310**, 384 (2002).
- ¹⁵E. E. Vogel, S. Contreras, J. Cartes, and J. Villegas, *Physics and Chemistry of Finite Systems: From Clusters to Crystals*, edited by P. Jena, S. N. Khana, and B. K. Rao (Kluwer Academic, Amsterdam, 1992), p. 813.
- ¹⁶E. E. Vogel, J. Cartes, S. Contreras, W. Lebrecht, and J. Villegas, *Phys. Rev. B* **49**, 6018 (1994).
- ¹⁷J. P. Sethna, K. Dahmen, S. Kartha, J. A. Krumhansl, B. W. Roberts, and J. D. Shore, *Phys. Rev. Lett.* **70**, 3347 (1993).
- ¹⁸E. Vives and A. Planes, *Phys. Rev. B* **50**, 3839 (1994).
- ¹⁹J. Kushauer, R. van Bentum, and W. Kleemann, *Phys. Rev. B* **53**, 11 647 (1996).
- ²⁰G. Alejandro, D. G. Lamas, L. B. Steren, J. E. Gayone, G. Zampieri, A. Caneiro, M. T. Causa, and M. Tovar, *Phys. Rev. B* **67**, 064424 (2003).